Analogue Models of Rocking Suitcases and Snaking Trailers

Zoltan Horvath and Denes Takacs

Abstract A mechanical model is constructed for the stability analysis of two-wheeled suitcases and trailers. The main assumptions of the model are summarized and the linearized equations of motion are presented. The linear stability of the rectilinear motion is investigated, critical parameter values are determined for the different level of complexity of the model. Numerical simulations are used to verify the applicability of the model for the nonlinear analysis of the rocking motion of trailers.

Keywords Two-wheeled suitcase · Trailer · Non-smooth system · Non-holonomic system

1 Introduction

The instability of towed vehicles (e.g. trailers, semi-trailers) is a relevant safety risk in road transport. Namely, under certain conditions (badly chosen load conditions and speed), a snaking motion may appear (see [1, 2]), which can even lead to the rocking motion of the trailer when it jumps from one of its wheels to the other. As a final result, the linear instability of the rectilinear motion of the trailer may cause the roll-over of the vehicle. This phenomenon can also be observed in case of a towed two-wheeled suitcase (see [3–6]), moreover similar mechanical models can be composed for the investigations of the stability behaviour. The analogies of the problems and the mechanical models are illustrated in Fig. 1.

Z. Horvath (✉)
Department of Applied Mechanics, Budapest University of Technology and Economics, Budapest, Hungary
e-mail: horvath.hanna.zsofia@gmail.com

D. Takacs
MTA-BME Research Group on Dynamics of Machines and Vehicles, Budapest, Hungary
e-mail: takacs@mm.bme.hu

W. Lacarbonara et al. (eds.), *Nonlinear Dynamics of Structures, Systems and Devices*, https://doi.org/10.1007/978-3-030-34713-0_12

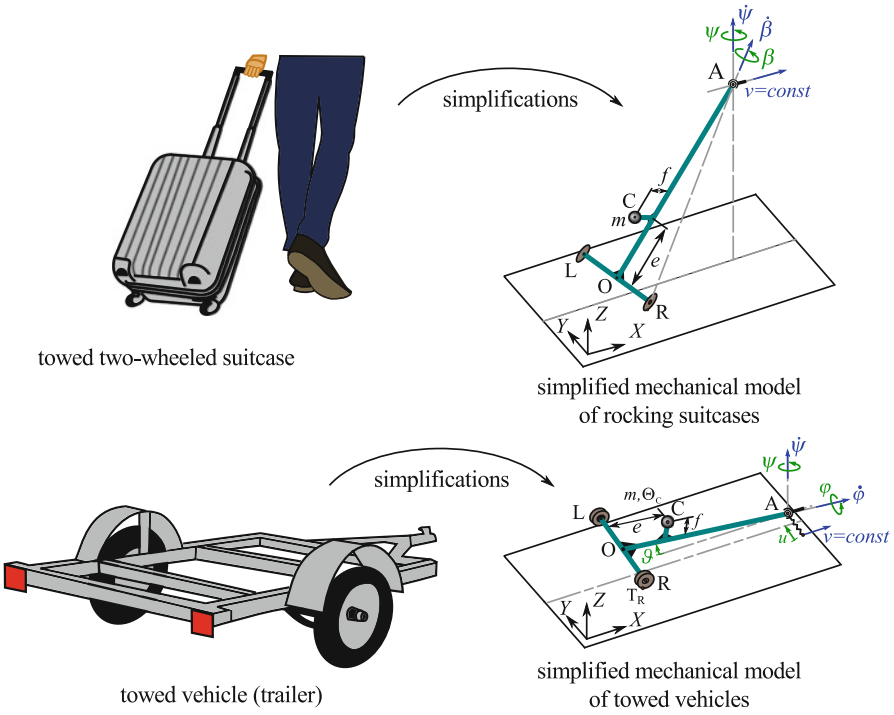

Fig. 1 Illustration of the analogy between rocking suitcases and snaking trailers with respect to their mechanical models

In our former study, we used the mechanical model of the rocking suitcase shown in the right top panel of Fig. 1 to analyse the linear stability and the basis of attraction of the rectilinear motion by means of numerical simulations and experiments (see [7]). The most exciting problem in the analysis of the mechanical model arises in the fact that governing equations of the mechanical model are non-smooth since different equations of motion describe the motion states of the suitcase (namely, when both wheels are on the ground, left or right wheel is on the ground, none of the wheels is on the ground). In addition, a kinematic constraint can be defined for the rolling wheels having point-like contact with the ground. The switching between the motion states is a complex task since switching appears when one of the wheels has an impact with the ground or when one of the wheels leaves the ground. Nevertheless, by implementing the mechanical model with its intricate non-smooth properties in a simulation code, one can investigate the effects of the initial conditions (e.g. initial tilting angle) and the different parameters (e.g. towing speed v, geometrical parameters e and f).

Of course, similar investigation can be done experimentally. A model-based experimental setup was also built and placed on a conveyor belt in [7]. The towed suitcase was perturbed at its left wheel by placing a cylindrical obstacle (with

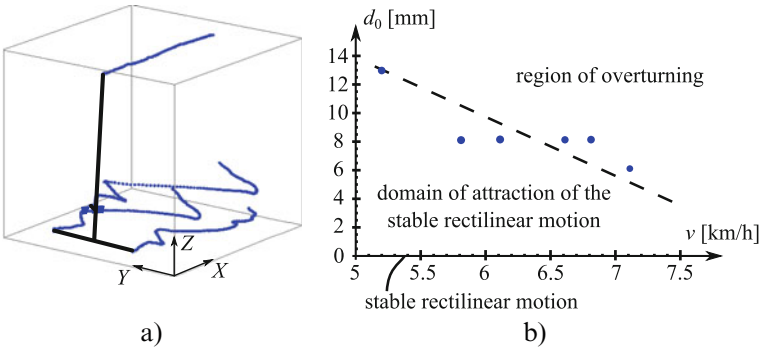

Fig. 2 (**a**) The trajectories of the retro-reflective markers attached to the suitcase at left and the right wheels, the centre of mass and the towing point, (**b**) basis of attraction of the rectilinear motion identified by experiments.

diameter d_0) onto to conveyor belt, and the motion of the suitcase was recorded by a motion capturing system using retro-reflective markers (see the left panel of Fig. 2). The detected basis of attraction of the rectilinear motion and its dependence on the towing speed can be seen in the right panel Fig. 2, where blue dots refer to the measurement points and dashed line illustrates the boundary of the basis of attraction. Both the numerical and experimental results confirmed that the attractive domain is smaller for larger speeds. In this study, we modify the mechanical model of the rocking suitcase to make it suitable for the analysis of the stability problem of trailers. In order to do this, the elasticities of the tyres and the wheel suspension system are taken into account. Although these modifications increase the degrees of freedom and the number of the parameters of the model, the mechanical model turns to be holonomic and the motion can be described uniquely with the same generalized coordinates independently from the actual motion state. After the short summary of the derivation of the equations of motion, the linear stability of the rectilinear motion is shown in the paper and numerical simulations are carried out to verify the applicability of the constructed mechanical model for the investigation of the nonlinear dynamics of rocking trailers.

2 Mechanical Model of Snaking Trailers

The mechanical model of snaking trailers can be seen on the left panel of Fig. 3. The motion of the trailer can be described with the yaw angle ψ, the pitch angle ϑ, the roll angle φ and the lateral displacement u of the joint at point A. Thus, the system has $n = 4$ degrees of freedom (DoF), the vector of the generalized coordinates is

$$\mathbf{q} = \left[\psi \ \vartheta \ \varphi \ u \right]^{\mathrm{T}} . \tag{1}$$

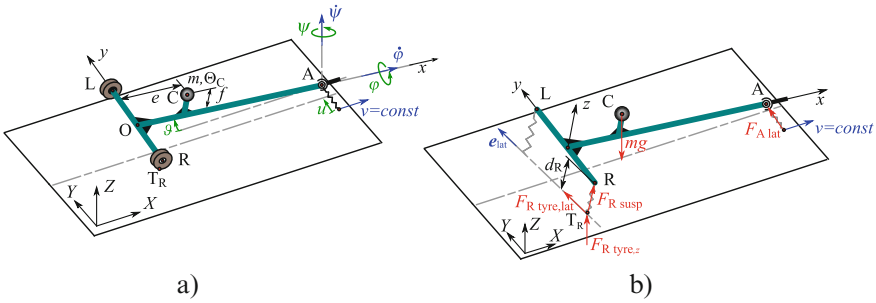

Fig. 3 (**a**) The mechanical model, (**b**) active forces acting on trailer

The towing length and the track width of the trailer are denoted by l and $2b$, respectively. The position of the centre of mass C can be described with parameters e and f. The overall stiffness and damping of the wheel suspension and tyres are denoted by k and c, while the lateral stiffness and damping at point A are k_l and c_l. The equations of motion can be derived with the Lagrange equation of the second kind:

$$\frac{\mathrm{d}}{\mathrm{d}t}\frac{\partial T}{\partial \dot{q}_k} - \frac{\partial T}{\partial q_k} = Q_k, \quad k = 1, \ldots, n\,, \tag{2}$$

where T is the kinetic energy, q_k is the kth generalized coordinate and Q_k is the kth component of the generalized force. The kinetic energy is calculated as

$$T = \frac{1}{2} m {v_\mathrm{C}}^2 + \frac{1}{2}\boldsymbol{\omega}^\mathrm{T}\boldsymbol{\Theta}_\mathrm{C}\boldsymbol{\omega}\,, \tag{3}$$

where the velocity of point C is $v_\mathrm{C} = |\mathbf{v}_\mathrm{C}| = |\mathbf{v}_\mathrm{A} + \boldsymbol{\omega} \times \mathbf{r}_\mathrm{AC}|$. The velocity of the towing point is $\mathbf{v}_\mathrm{A} = [\,v\ \dot{u}\ 0\,]^\mathrm{T}$ given in the ground fixed (X, Y, Z) coordinate system. The angular velocity of the trailer given in the trailer fixed (x, y, z) coordinate system is

$$\boldsymbol{\omega} = \begin{bmatrix} \dot{\varphi} - \dot{\psi}\sin\vartheta \\ \dot{\vartheta}\cos\varphi + \dot{\psi}\cos\vartheta\sin\varphi \\ \dot{\psi}\cos\vartheta\cos\varphi - \dot{\vartheta}\sin\varphi \end{bmatrix}_{(x,y,z)}. \tag{4}$$

Let us consider the mass moment of inertia matrix as

$$\boldsymbol{\Theta}_\mathrm{C} = \begin{bmatrix} \Theta_{\mathrm{C},x} & 0 & 0 \\ 0 & \Theta_{\mathrm{C},y} & 0 \\ 0 & 0 & \Theta_{\mathrm{C},z} \end{bmatrix}_{(x,y,z)}. \tag{5}$$

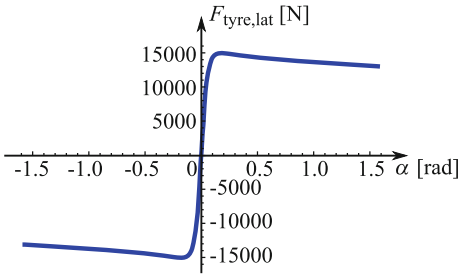

Fig. 4 The characteristics of the tyre forces in case of $F_z = 15{,}000$ N. The factors: $B = 10$ (stiffness factor), $C = 1.9$ (shape factor), $D = 1$ (peak factor), $E = 0.97$ (curvature factor)

The generalized force can be obtained from the virtual power:

$$\begin{aligned}\delta P = \mathbf{G} \cdot \delta \mathbf{v}_{\mathrm{C}} + \mathbf{F}_{\mathrm{R}_{\mathrm{tyre}}} \cdot \delta \mathbf{v}_{\mathrm{T_R}} + \mathbf{F}_{\mathrm{R}_{\mathrm{susp}}} \cdot \delta \mathbf{v}_{\mathrm{R}} + \mathbf{F}_{\mathrm{L}_{\mathrm{tyre}}} \cdot \delta \mathbf{v}_{\mathrm{T_L}} \\ + \mathbf{F}_{\mathrm{L}_{\mathrm{susp}}} \cdot \delta \mathbf{v}_{\mathrm{L}} + \mathbf{F}_{\mathrm{A}_{\mathrm{lat}}} \cdot \delta \mathbf{v}_{\mathrm{A}} \,,\end{aligned} \tag{6}$$

where $\mathbf{G}$ is the gravitational force, $\mathbf{F}_{\mathrm{R}_{\mathrm{tyre}}}$ and $\mathbf{F}_{\mathrm{L}_{\mathrm{tyre}}}$ represent the forces acting on the tyres at points $\mathrm{T_R}$ and $\mathrm{T_L}$. $\mathbf{F}_{\mathrm{R}_{\mathrm{susp}}}$ and $\mathbf{F}_{\mathrm{L}_{\mathrm{susp}}}$ are the forces acting on the chassis of the trailer at points R and L due to the elastic deformation of the suspensions. $\mathbf{F}_{\mathrm{A}_{\mathrm{lat}}}$ is the lateral force acting at point A. These forces are shown in the right panel of Fig. 3.

The tyre forces can be calculated with the help of the Magic Formula of Pacejka (see [8]):

$$F_{\text{tyre,lat}}(\alpha, F_z) = F_z D \sin\left(C \arctan\left(B\alpha - E\left(B\alpha - \arctan(B\alpha)\right)\right)\right) \,, \tag{7}$$

where B, C, D, E are the tyre parameters and F_z is the vertical load on the tyre. The tyre force characteristics can be seen in Fig. 4. The side slip angle of the right wheel can be calculated as

$$\alpha_{\mathrm{R}} = -\arctan\left(\frac{\mathbf{v}_{\mathrm{T_R}} \cdot \mathbf{e}_{\mathrm{lat}}}{\mathbf{v}_{\mathrm{T_R}} - (\mathbf{v}_{\mathrm{T_R}} \cdot \mathbf{e}_{\mathrm{lat}})\mathbf{e}_{\mathrm{lat}}}\right) \,, \tag{8}$$

where unit vector $\mathbf{e}_{\mathrm{lat}}$ refers to the lateral direction of the trailer projected to the ground. The side slip angle of the left wheel can be calculated similarly.
The force originated in the wheel suspension acts on the trailer in the z direction, its magnitude is

$$\begin{aligned}F_{\mathrm{R\,susp}} = \left((L_{\mathrm{R},0} - d_{\mathrm{R}})k + (v_{\mathrm{T_R},z} - v_{\mathrm{R},z})c\right) \cdot H(L_{\mathrm{R},0} - d_{\mathrm{R}}) \\ \cdot H((L_{\mathrm{R},0} - d_{\mathrm{R}})k + (v_{\mathrm{T_R},z} - v_{\mathrm{R},z})c)\end{aligned} \tag{9}$$

for the right wheel, where the Heaviside-function $H(x) = (1 + \tanh(x/\varepsilon))/2$ with the smoothing parameter ε is used to make the system to be smooth. The parameter

$L_{\mathrm{R},0}$ is the free length of the spring while d_{R} is the actual length of the spring (see panel (b) in Fig. 3). The force originated in the left wheel suspension can be calculated similarly.

3 Linear Stability Analysis

The rectilinear motion of the trailer corresponds to: $\psi(t) \equiv \psi_0 = 0$, $\vartheta(t) \equiv \vartheta_0 = 0$, $\varphi(t) \equiv \varphi_0 = 0$, $u(t) \equiv u_0 = 0$ in case of the spring free length $L_{\mathrm{R},0} \equiv L_{\mathrm{L},0} = h + mg(l-e)/(2kl)$. The linearized equation of motion can be written as

$$\mathbf{M}\ddot{\mathbf{q}} + \mathbf{C}\dot{\mathbf{q}} + \mathbf{K}\mathbf{q} = \mathbf{0}\,, \tag{10}$$

where the mass matrix is

$$\mathbf{M} = \begin{bmatrix} m(e-l)^2 + \Theta_{\mathrm{C},z} & 0 & mf(l-e) & m(e-l) \\ 0 & mf^2 + m(e-l)^2 + \Theta_{\mathrm{C},y} & 0 & 0 \\ mf(l-e) & 0 & mf^2 + \Theta_{\mathrm{C},x} & -mf \\ m(e-l) & 0 & -mf & m \end{bmatrix}, \tag{11}$$

the damping matrix is

$$\mathbf{C} = \begin{bmatrix} \frac{BCDmgl(l-e)}{v} & 0 & \frac{BCDmgh(e-l)}{v} & \frac{BCDmg(e-l)}{v} \\ 0 & 2cl^2 & 0 & 0 \\ \frac{BCDmgh(e-l)}{v} & 0 & \frac{2b^2clv+BCDmgh^2(l-e)}{lv} & \frac{BCDmgh(e-l)}{lv} \\ \frac{BCDmg(e-l)}{v} & 0 & \frac{BCDmgh(e-l)}{lv} & \frac{c_1lv+BCDmgh^2(l-e)}{lv} \end{bmatrix} \tag{12}$$

and the stiffness matrix is

$$\mathbf{K} = \begin{bmatrix} BCDmg(l-e) & 0 & mg(e-l) & 0 \\ 0 & 2l^2k - mgf & 0 & 0 \\ \frac{BCDmgh(e-l)}{l} & 0 & 2b^2k - mgf & 0 \\ \frac{BCDmgh(e-l)}{l} & 0 & \frac{mg(l-e)}{l} & k_1 \end{bmatrix}. \tag{13}$$

It is worth to notice that the stiffness matrix is asymmetric. As it can be seen, the system can be separated into two subsystems: the second component of (10) corresponding to the pitch motion can be separated, the other equations are coupled ($n = 3$ DoF subsystem).

3.1 The Pitch Motion of the Trailer

The equation of motion of the separable subsystem is a second-order ordinary differential equation, from which the critical value of the stiffness k can be expressed:

$$k_{\mathrm{cr}} = \frac{mgf}{2l^2}\,. \tag{14}$$

This critical value corresponds to static loss of stability, namely the trailer overturns about the lateral axis for $k < k_{\mathrm{cr}}$.

3.2 The Yaw and Roll Motion of the Trailer

The equations of motion of the coupled subsystem consist of three second-order ordinary differential equations. By using the trial solution

$$\mathbf{q} = \mathbf{A}\mathrm{e}^{\lambda t} \tag{15}$$

with the characteristic root λ, the characteristic equation becomes

$$\det\left(\lambda^2\mathbf{M} + \lambda\mathbf{C} + \mathbf{K}\right) = 0\,. \tag{16}$$

The stability of the rectilinear motion can be investigated by Routh–Hurwitz criteria. Unfortunately, no closed form expression can be given for the critical parameter values in general case. But for $k_{\mathrm{l}} \to \infty$ (i.e. when the joint at A is laterally rigid), the system simplifies to a $n = 3$ DoF system and critical stiffness values can be determined for the undamped ($c = 0$) case:

$$k_{\mathrm{cr},1} = \frac{mg(l(f+h) - eh)}{2b^2 l}\,, \tag{17}$$

and

$$k_{\mathrm{cr},2} = \frac{mgl^2\left(l(e-l)\Theta_{\mathrm{C},x} + fh\Theta_{\mathrm{C},z}\right)}{2b^2l^2\left(me^2h - mel(f+2h) + mfl^2 + h\left(\Theta_{\mathrm{C},z} + ml^2\right)\right)} - \frac{mgBCDh(e-l)\left(me^2h^2 - 2mehl(f+h) + h^2\Theta_{\mathrm{C},z} + ml^2(f+h)^2 + \Theta_{\mathrm{C},x}l^2\right)}{2b^2l^2\left(me^2h - mel(f+2h) + mfl^2 + h\left(\Theta_{\mathrm{C},z} + l^2m\right)\right)}\,. \tag{18}$$

Static stability loss occurs if $k < k_{\mathrm{cr},1}$, namely the trailer falls over. Dynamic loss of stability happens if $k_{\mathrm{cr},1} < k < k_{\mathrm{cr},2}$, and the rectilinear motion is stable for $k_{\mathrm{cr},2} < k$. These critical values can be also identified by the numerical calculation

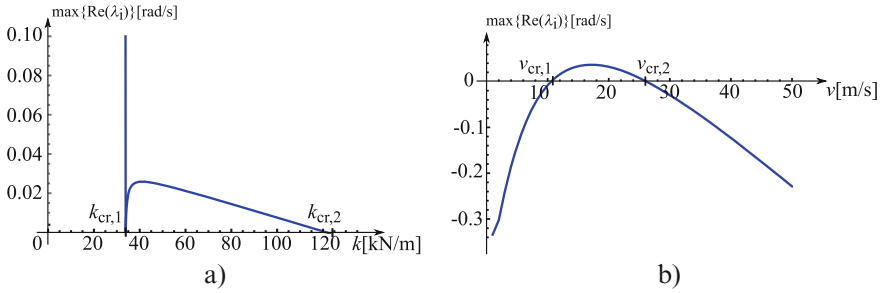

Fig. 5 The real part of the rightmost characteristic root of the linearized system. (**a**) Critical spring stiffness values for the 3 DoF model, (**b**) unstable speed range in case of the 4 DoF model. Parameter values: $l = 3\,\text{m}$, $b = 0.8\,\text{m}$, $e = 1\,\text{m}$, $f = 1\,\text{m}$, $h = 0.5\,\text{m}$, $m = 3000\,\text{kg}$, $k = 60{,}000\,\text{N/m}$, $c = 6000\,\text{Ns/m}$, $B = 10$, $C = 1.9$, $D = 1$, $E = 0.97$, (**a**) $k_1 \to \infty$, (**b**) $k_1 = 10{,}000\,\text{N/m}$, $c_1 = 100\,\text{Ns/m}$

of the characteristic roots, see panel (a) of Fig. 5, where the real part of the rightmost characteristic root is plotted versus the stiffness.

Of course, the linear stability of original four degree-of-freedom mechanical model can also be investigated numerically. Panel (b) of Fig. 5 shows the real part of the rightmost characteristic root versus the towing speed v. For a certain velocity range (approx. between 10 and 26 m/s), the rectilinear motion is unstable.

4 Simulation

Numerical simulations were run in order to verify the critical parameter values given by the linear stability analysis and to check the nonlinear dynamics of the trailer. Fourth order Runge–Kutta method was used with fix time step. The simulations were run for different initial conditions and for different spring stiffness values (3 DoF model) or for different towing velocity values (4 DoF model). Here we present only a simulation result for $k_1 \to \infty$ and for $k = 75{,}000\,\text{N/m}$. As it can be seen, the motion tends to a large amplitude rocking motion, see Fig. 6.

Based on the numerical simulations, one can also draw the bifurcation diagram of the four degree-of-freedom system. The top left panel of Fig. 7 depicts the amplitude of the roll angle with respect to the bifurcation parameter v. Subcritical Hopf bifurcation is suspected, which could be validated by using a bifurcation software. Panel (b) of Fig. 7 shows the effects of parameters f and e on the linear stability of the rectilinear motion. The red areas correspond to linearly unstable rectilinear motion (snaking, rocking, roll-over of the trailer may appear), while the green areas correspond to linearly stable rectilinear motion.

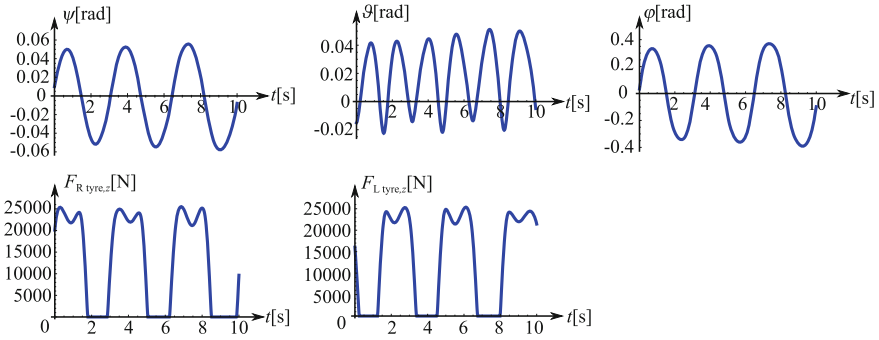

Fig. 6 The time histories of the generalized coordinates and the vertical forces acting on the left or the right wheel in case of $k = 75{,}000\,\text{N/m}$

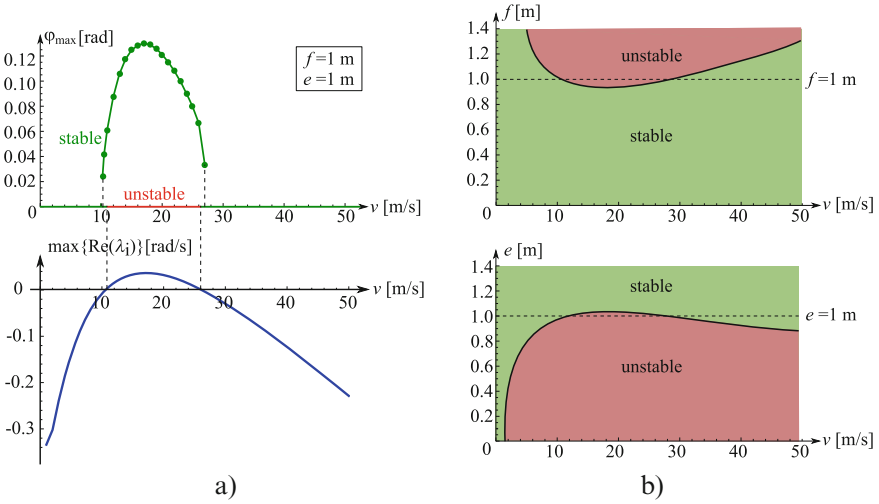

Fig. 7 (**a**) The bifurcation diagram of the four degree-of-freedom system, in case of $k = 75{,}000\,\text{N/m}$ (top panel) and the real part of the rightmost characteristic root of the linearized system (bottom panel). (**b**) The effects of parameters f and e on the linear stability of the rectilinear motion. The green areas correspond to linearly stable, the red areas correspond to linearly unstable motion

5 Conclusions

A mechanical model was introduced by which both the stability of two-wheeled suitcases and trailers can be investigated. It was shown that the linear stability of the rectilinear motion depends on the speed if the lateral displacement of the towing joint is considered. Critical stiffness values were also determined for the wheel suspensions. Simulation results also confirmed that the model can exhibit the

large amplitude rocking motion and the nonlinear analysis of the model may lead to relevant information about the instability of the trailer.

Acknowledgements This research has been supported by the UNKP-18-2-I-BME-173 New National Excellence Program of the Ministry of Human Capacities Hungary. This research was funded by the National Research, Development and Innovation Office under grant no. NKFI-128422. The publication of the work reported herein has been supported by ETDB at BME.

References

1. Troger, H., Zeman, K.: A nonlinear-analysis of the generic types of loss of stability of the steady-state motion of a tractor-semitrailer. Veh. Syst. Dyn. **13**(4), 161–172 (1984)
2. Darling, J., Tilley, D., Gao, B.: An experimental investigation of cartrailer high-speed stability. Proc. Inst. Mech. Eng. D: J. Autom. Eng. **223**(4), 471–484 (2009)
3. Suherman, S., Plaut, R.H., Watson, L.T., Thompson, S.: Effect of human response time on rocking instability of a two-wheeled suitcase. J. Sound Vib. **207**(5), 617–625 (1997)
4. Plaut, R.H.: Rocking instability of a pulled suitcase with two wheels. Acta Mech. **117**, 165–179 (1996)
5. O'Reilly, O.M., Varadi, P.C.: A travelers woes: some perspectives from dynamical systems. In: Moon, F.C. (ed.) IUTAM Symposium on New Applications of Nonlinear and Chaotic Dynamics in Mechanics Kluwer, Dordrecht, pp. 397–406 (1999)
6. Facchini, G., Sekimoto, K., Courrech du Pont, S.: The rolling suitcase instability: a coupling between translation and rotation. Proc. R. Soc. A: Math. Phys. Eng. Sci. **473**(2202), 20170076 (2017)
7. Horvath, H.Zs., Takacs, D.: Modelling and Simulation of Rocking Suitcases. Acta Polytech. CTU Proc. **18**, 61–65 (2018). https://doi.org/10.14311/APP.2018.18.0061
8. Pacejka, H.B.: Tyre and Vehicle Dynamics, Elsevier Butterworth-Heinemann, Oxford (2002)